the plant journal

SEB Society for Experimental Biology

The Plant Journal (2014) **77,** 676–687 doi: 10.1111/tpj.12418

Silencing of the tomato Sugar Partitioning Affecting protein (SPA) modifies sink strength through a shift in leaf sugar metabolism

Luisa Bermúdez[1,2,†], Fabiana de Godoy[1,†], Pierre Baldet[3], Diego Demarco[1], Sonia Osorio[4,§], Leandro Quadrana[2,5], Juliana Almeida[1], Ramón Asis[5,6], Yves Gibon[3], Alisdair R. Fernie[4], Magdalena Rossi[1,‡] and Fernando Carrari[2,5,‡,*]

[1]*Departamento de Botânica, Instituto de Biociências, Universidade de São Paulo, Rua do Matão, 277, São Paulo, 05508-900 SP, Brazil,*

[2]*Instituto de Biotecnología, Instituto Nacional de Tecnología Agropecuaria (IB-INTA), PO Box 25, Castelar B1712WAA, Argentina,*

[3]*INRA-Bordeaux, Fruit Biology and Pathology Unit, Villenave d'Ornon F-33883, France,*

[4]*Max Planck Institute of Molecular Plant Physiology, Wissenschaftspark Golm, Am Mühlenberg 1, Potsdam-Gölm, D-14476, Germany,*

[5]*Consejo Nacional de Investigaciones Científicas y Técnicas (CONICET), PO Box 25, Castelar B1712WAA, Argentina, and*

[6]*CIBICI, Facultad de Ciencias Químicas Universidad Nacional de Córdoba, Córdoba CC 5000, Argentina*

Received 13 July 2012; revised 3 December 2013; accepted 10 December 2013; published online 30 December 2013.

*For correspondence (e-mail fcarrari@cnia.inta.gov.ar).

†These authors contributed equally to this work.

‡These authors contributed equally to this work.

§Present address: Departamento de Biología Molecular y Bioquímica, Instituto de Hortofruticultura Subtropical y Mediterránea (IHSM), Universidad de Málaga-Consejo Superior de Investigaciones Científicas, Málaga, 29010, Spain.

SUMMARY

Limitations in our understanding about the mechanisms that underlie source-sink assimilate partitioning are increasingly becoming a major hurdle for crop yield enhancement via metabolic engineering. By means of a comprehensive approach, this work reports the functional characterization of a DnaJ chaperone related-protein (named as *SPA*; *sugar partition-affecting*) that is involved in assimilate partitioning in tomato plants. SPA protein was found to be targeted to the chloroplast thylakoid membranes. *SPA*-RNAi tomato plants produced more and heavier fruits compared with controls, thus resulting in a considerable increment in harvest index. The transgenic plants also displayed increased pigment levels and reduced sucrose, glucose and fructose contents in leaves. Detailed metabolic and enzymatic activities analyses showed that sugar phosphate intermediates were increased while the activity of phosphoglucomutase, sugar kinases and invertases was reduced in the photosynthetic organs of the silenced plants. These changes would be anticipated to promote carbon export from foliar tissues. The combined results suggested that the tomato SPA protein plays an important role in plastid metabolism and mediates the source-sink relationships by affecting the rate of carbon translocation to fruits.

Keywords: tomato, small plastidial protein, fruit metabolism, source-sink partitioning, chloroplast metabolism.

INTRODUCTION

In the past decades, improvement of crop yields has been achieved principally by the use of fertilizers, expanded irrigation and integrated pest management. As a consequence, however, a detrimental impact on sustainability and environmental quality is currently being evidenced (Tilman *et al.*, 2011). In addition to these strategies, plant breeding efforts to increase yield directly per hectare, which are principally aimed at the enhancement of harvest index (HI), have been attempted (Lippman *et al.*, 2007; Yang and Zhang, 2010). Food and bioenergy production must increase substantially in the next years in order to supply the increasing global demand for these commodities. That said, increasing HI by modulation of assimilate partitioning alone, whilst working in some cases, will probably fail due to limitations in sink tissues' capacity to capitalize on the increased availability of photosynthate.

Considerable experimental data have suggested that photosynthesis is controlled by whole plant source-sink balance that involves carbon to nitrogen status and nutrient availability (Paul and Foyer, 2001). To date, with a few exceptions, the efforts to increase the partitioning of fixed carbon into harvestable sinks have been restricted largely to the manipulation of carbon fluxes via the modification of individual enzymatic steps (reviewed in Nunes-Nesi *et al.*, 2011); results have been largely unsuccessful (Roitsch, 1999). This situation is mostly due to our limited knowledge of the signals that communicate source and sink organs, despite the fact that a comprehensive understanding of the underlying mechanisms is being pursued actively (Paul and Foyer, 2001; Paul and Pellny, 2003; Nunes-Nesi *et al.*, 2010).

Recently, Schauer *et al.* (2006) performed quantitative trait loci (QTL) analysis on a set of well characterized tomato introgression lines (Eshed and Zamir, 1995). Further analyses of the data, from a network perspective, revealed that a many metabolic changes in mature fruits were connected strongly to yield-associated traits – most prominently to HI. A survey of the genomic regions that spanned those QTL located to tomato chromosome 4 (BIN 4I) identified nine candidate genes, four of which only encoded enzyme-related functions (Bermúdez *et al.*, 2008). A DnaJ chaperone-like encoding gene that mapped within the genomic region that spanned these QTL (Bermúdez *et al.*, 2008) and its mRNA profile correlated with variations in a wide range of primary metabolites across tomato fruit development (Carrari *et al.*, 2006). Thus, this protein, subsequently named *sugar partitioning-affecting* (*SPA*), appeared to be a candidate involved in some of the observed metabolic changes. Chaperone proteins of this type have been shown to regulate thylakoid biogenesis in cotyledons (Shimada *et al.*, 2007), act as redox switches for the reorganization of regulatory protein complexes (Dorn *et al.*, 2010), and regulate photosynthetic reactions (Chen *et al.*, 2010) in Arabidopsis plants. The DnaJ family of molecular chaperones has been identified in diverse organisms and cellular compartments. It has been demonstrated that several members of this protein family are involved in critical processes that included protein folding, unfolding and assembly, under both normal and stress conditions (Chen *et al.*, 2010; Li *et al.*, 2012). In Arabidopsis, 26 DnaJ proteins have been predicted to be localized to the chloroplast and participate mainly in division and plastid biogenesis processes (Vitha *et al.*, 2003; Chen *et al.*, 2010, 2011). To gain further insight about the role of this protein in tomato, here we present the functional characterization of the *SPA* gene. The integrated analysis of a comprehensive set of data including gene structure, protein localization, expression profile and a deep phenotyping of *SPA*-silenced tomato plants demonstrated that SPA participates in determining HI in tomato by affecting source-sink carbon distribution through a mechanism that involves the regulation of phosphoglucomutase, sugar kinase and invertase enzyme activities. Thus, results presented here allow us to propose SPA as a target for plant metabolic engineering by showing an unprecedented function for this protein family.

RESULTS

Gene characterization; phylogeny and expression

SPA, a DnaJ-like protein encoding gene, was identified as a candidate gene associated with several fruit metabolic QTL (namely amino and organic acids and sugar content variations) mapped in a *Solanum pennellii* (accession LA716) introgression line population in a domesticated genetic background (*S. lycopersicum* cv. M82). A detailed evaluation of both alleles of this gene revealed that *SPA* mRNA spans 3019 and 3063 nucleotides (nt) for *S. pennellii* (*Sp-SPA)* and *S. lycopersicum* (*Sl-SPA*) alleles, respectively. The alleles shared conserved structures with five exons that, nevertheless, differ in few single nucleotide polymorphisms (SNPs) and small insertion/deletions (InDels). However, within the coding regions, only SNPs were identified that resulted in two amino acids differences within the predicted chloroplast transit peptide (TP). One of these polymorphisms altered the predicted cleavage site and resulted in a TP with 65 amino acids (aa) in the *Sl-SPA* allele and 47 aa in the *Sp-SPA* one. The full peptide comprised a 159 aa chain that exhibited a transmembrane (TM) domain and a canonical DnaJ-zinc-finger domain (Figure 1a).

Phylogenetic analysis that included other DnaJ-like genes whose functions have been previously demonstrated experimentally, revealed that these proteins present a wide and diverse domain repertoire; five clades can be distinguished according to their protein structure. *Sp*-SPA and *Sl*-SPA clustered together with the corresponding Arabidopsis ortholog (At-LQY1), (Lu *et al.*, 2011; Figure 1b).

The predicted sub-cellular localization was confirmed by transient expression experiments in which both coding regions, *Sp-SPA and Sl-SPA*, were fused to the green fluorescent protein (*GFP*) reporter gene under the control of the cauliflower mosaic virus (CaMV) 35S promoter. *Agrobacterium* cultures that carried the fusion proteins were infiltrated into *Nicotiana benthamiana* leaves and, after 48 h, GFP fluorescence was evaluated by confocal microscopy. GFP fluorescence was detected co-incident with chlorophyll auto-fluorescence (Figure 1c), and suggested plastidial location of SPA protein. Moreover, chloroplast fractionation and subsequent western blot analyses allowed us to determine that SPA is localized mainly in thylakoid membranes (Figure 1d).

To gain further insight into the putative role of SPA in the above-mentioned metabolic variations, its gene expression pattern was evaluated by qPCR both in cv. M82

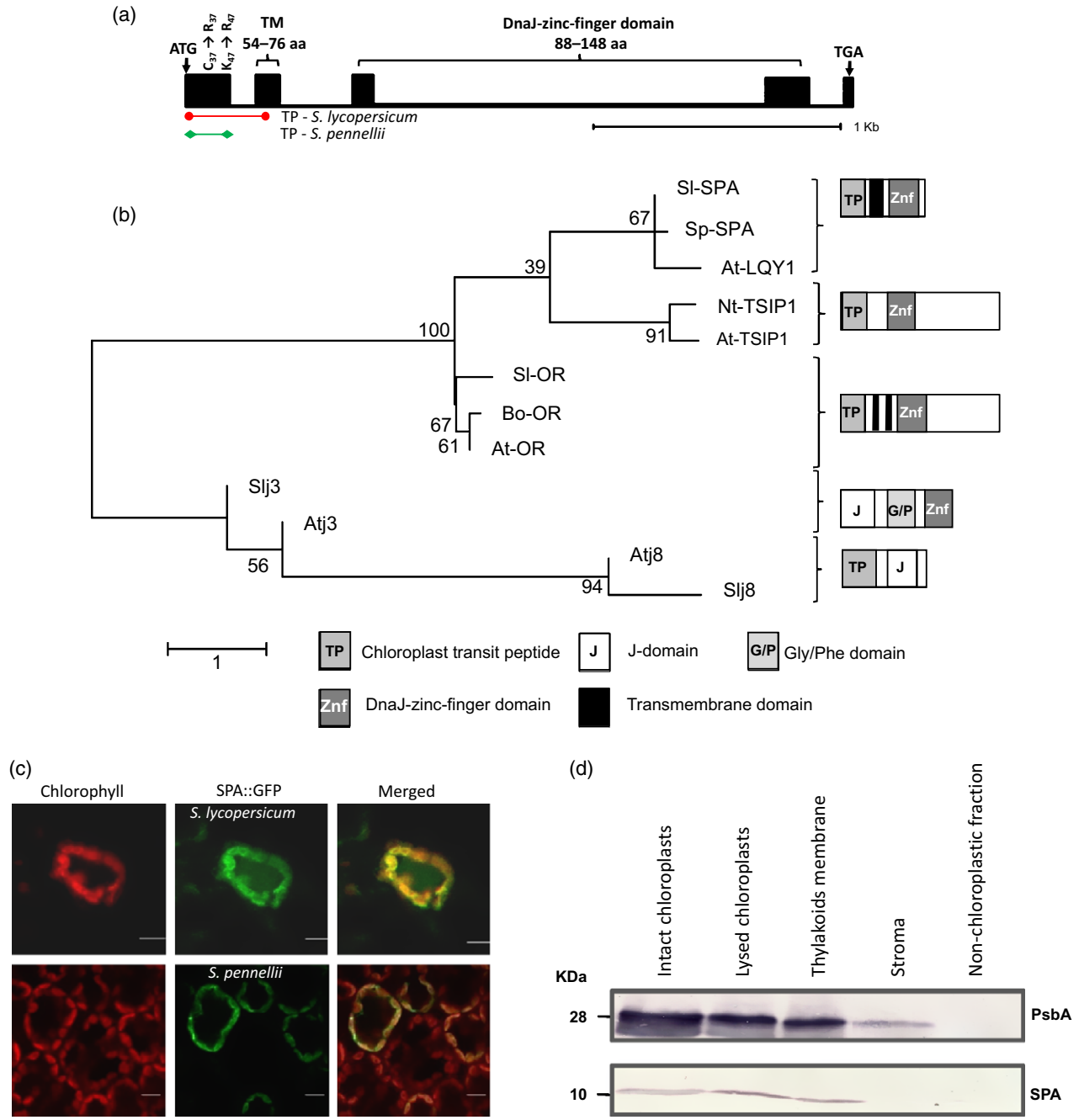

Figure 1. Structure of the tomato *SPA* gene and protein localization.
(a) Gene structure and protein domains based on DNA sequence analysis. Black boxes and lines represent exons and intron, respectively. The start and stop codons, and the amino acid polymorphisms between *S. lycopersicum* and *S. pennellii* alleles are indicated. TM, transmembrane domain; TP, chloroplast transit peptide.
(b) Phylogenetic tree of previously functional characterized DnaJ homologs in plants. For each clade was included the characterized gene, Arabidopsis and tomato homologs (when found), and the respective protein structure. Sequence accession numbers are indicated in Experimental Procedures. At: *A. thaliana*; Bo: *B. oleraceae*; Sl: *S. lycopersicum*; Sp: *S. pennellii* and Nt: *N. tabacum*.
(c) Confocal imaging of chlorophyll fluorescence and SPA::GFP fluorescence protein in mesophyll cells of *N. benthamiana* leaves. Merged: overlay of GFP (green) and chlorophyll (red) images showing the SPA localization in chloroplasts for both *S. pennellii* and *S. lycopersicum* alleles. Scale bar 10 μm.
(d) Western blot of SPA protein in fractionated chloroplasts from wild-type (cv. MoneyMaker) plants. Chloroplast proteins were probed with affinity-purified anti-LQY1 (SPA) and anti-thylakoid compartment marker (psbA/D1) antibodies. Each lane on the gel contains 40 μg of total proteins.

(carrying the domesticated *Sl-SPA* allele) and in IL4-4 (carrying the *Sp-SPA* allele). mRNA quantification revealed that *SPA* is minimally expressed in fruits and stems, but a significantly higher level of expression was detected in source leaves from the cultivated genotype (Figure 2a). To investigate whether this differential expression pattern

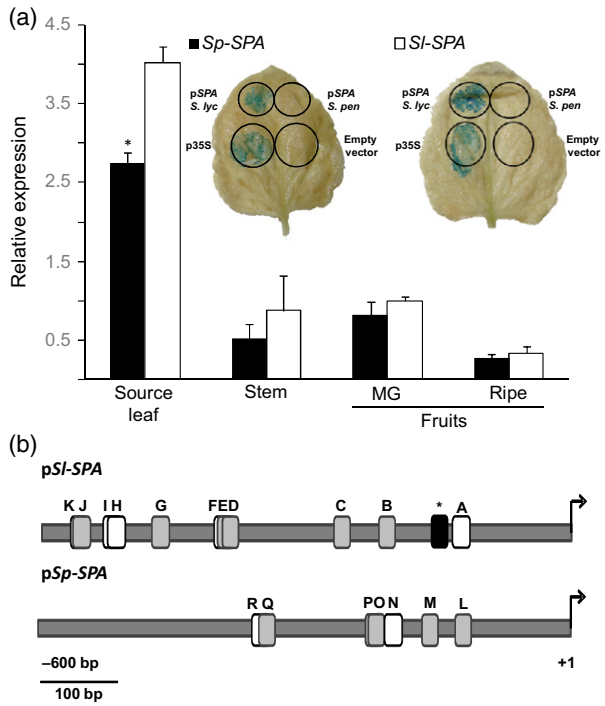

Figure 2. *Sl-* and *Sp-SPA* transcriptional activity.
(a) *SPA* expression profile by qPCR in source leaves, stem, and tomato fruit at two different ripening stages (MG, mature green and ripe) harvested from IL 4-4 (black bar) and *S. lycopersicum* (M82; white bar) genotypes. Data are expressed relative to *S. lycopersicum* mature green stage. GUS transient expression analyses after Agrobacterium infiltration with the promoter-*GUS* fusion construct in *N. benthamiana* leaves are shown in the inset. Upper-left circle: pHGWFS7-*SPA*-prom-S.lyc; upper-right circle: pHGWFS7-*SPA*-prom-S.pen; lower-left circle: pHGWFS7-35S and lower-right circle: pHGWFS7-empty vector. *Statistically significant differences at $P < 0.05$.
(b) Differential motifs in the *SPA* putative promoter region of *S. lycopersicum* and *S. pennellii* alleles. White and gray boxes indicate motifs in sense and antisense strands, respectively. Black box (*) represents a differential enhancer found in *S. lycopersicum* promoter. Motifs are named according to Table S1.

could be due to *cis*-regulatory mechanisms, a transient promoter activity assay was performed. The sequences upstream from the transcription start sites to the initiation of the neighboring gene were considered as putative promoter regions and were fused to the GUS reporter gene *uidA*. In agreement with the qPCR experiment, measurements of GUS activity suggest that the *S. lycopersicum* allele is transcribed more abundantly in source leaves (Figure 2a inset). Moreover, when the promoter regions were analyzed *in silico*, differential *cis*-motifs were detected in both alleles. Interestingly, a TA-rich region type of enhancer was identified exclusively in the *Sl-SPA* promoter (Figure 2b and Table S1).

SPA-silenced tomato plants display alterations in yield-associated traits

Analyses of RNA interference plants were carried out to improve our understanding of the role that the SPA protein could play in whole plant physiology. Twenty seven primary PCR (polymerase chain reaction)-positive independent transformants that expressed an RNAi triggering construct under the control of the CaMV 35S promoter, were screened for their SPA mRNA levels by qPCR. Four lines that displayed different silencing levels (named as RNAi:*SPA*-7, RNAi:*SPA*-12, RNAi:*SPA*-39, and RNAi:*SPA*-43) were selected for further phenotypic characterization. Silencing was confirmed in leaves and ripe fruits from six biological replicates of the selected T0 lines (Figure 3a,b) and further in the T1 segregants. No evident morphological alterations were observed in the transgenic plants. Although vegetative biomass was unaltered (Figure 3c), at harvest time both the weight of mature fruits (Figure 3d) and its number per plant (Figure 3e) increased in the silenced lines. As no differences were observed in the number of trusses per plant (four at harvest stage), the alteration in total fruit number was the result of a higher number of fruit per truss (2–4 and 4–8 for controls and transgenic plants, respectively). This fact was reflected by a significant increase in HI (Figure 3f).

SPA silencing affects sugar metabolism and pigment content without altering photosynthetic parameters

To better understand the origin of the observed changes in carbon allocation, we analyzed comparatively the metabolite profiles of source leaves and ripe fruits from the *SPA*-silenced plants (Figure 4, Tables S2 and S3). Interestingly, massive alterations in sugars and amino acids were detected, in source leaves. Sucrose, glucose and fructose decreased significantly, while xylose, ribose and rhamnose showed higher contents in the silenced lines. The amino acids displayed increments that ranged from 1.5- to 3.5-fold and were accompanied by increments in urea and aromatic amines (i.e. tyramine and putrescine). These changes were along with significant increments in the levels of oxo-glutarate, glycerate, ribonate and galactinol. A moderated decrease in the starch levels was also observed in the *SPA*-silenced lines. This change was also observed when registering the number of starch granules in photomicrographs of source leaves sections (Figure S1). In contrast, there were few metabolite changes in mature fruits (Figure 4b and Table S3). Regarding amino acids, only alanine and serine showed reduced levels, whilst phenylalanine showed significant increments in mature fruits of the transgenic lines. Levels of sucrose and citrate also decreased and trehalose increased in the transgenics. Although the observation of starch granules in fruit cells may indicate an evident increment in the transgenics (Figure S1c,d), total starch levels did not show significant differences from wild-type controls when measured by a quantitative technique (Table S3).

Photosynthetic parameters were measured in dark-adapted leaves of 4-week-old plants. Neither carbon assimilation nor stomatal conductance were affected in the silenced lines in comparison with wild-type controls at any

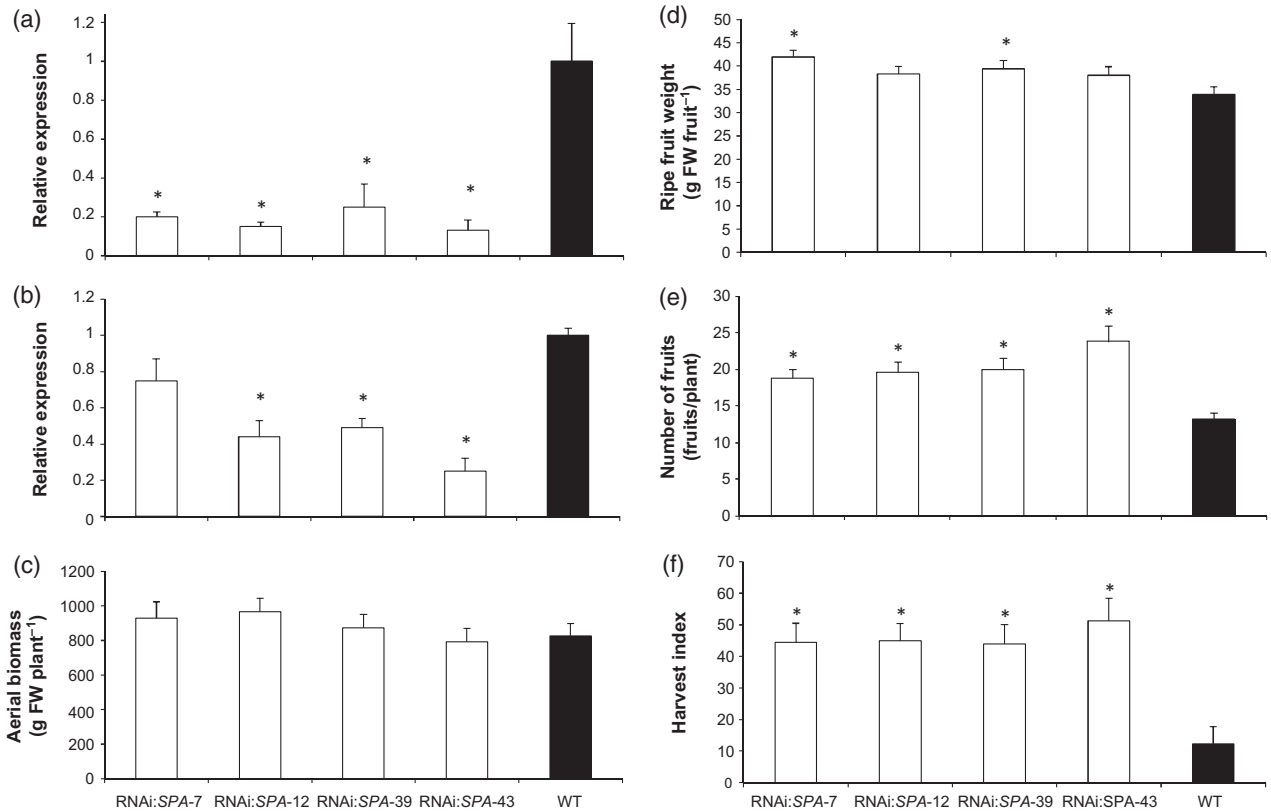

Figure 3. *SPA* expression and yield-associated traits in silenced transgenic lines.
SPA mRNA levels in source leaves (a) and mature fruits (b). Bars represent averages of three independent qPCR experiments from six (a) and three (b) biological replicates. Values are normalized to the constitutive EF1α gene expression and are expressed as the relative abundance of mRNA compared to wild-type control (cv. MoneyMaker).
(c–f) Data values are presented as mean ± SE from three to six individual plants per line at harvest stage (4-month-old plants). Harvest index = total fruit weight × 100/aerial biomass. *Statistically significant differences at $P < 0.05$.

of the photon flux densities tested (Table S4). This situation was also true for the chlorophyll fluorescence parameters. Even though leaf pigments (chlorophyll a, b and total carotenoids) were increased in *SPA*-silenced lines, no significant changes were observed in the contents of the major fruit pigments lycopene and β-carotene (Table 1). We also examined chloroplast ultrastructure of source leaves by transmission microscopy. Except for the size of the starch granules, which were smaller in the transgenics (in agreement with spectrophotometrical measurements), there were neither differences in the numbers nor in the shape of this organelle in the transgenic lines (Figure S2).

Taken together, these integrated analyses suggest that the observed increase in HI of the *SPA*-silenced plants is more related to an altered distribution of photoassimilates than to impairments in carbon assimilation.

SPA silencing affects the activities of carbohydrate metabolism enzymes and triose- and hexose-P contents in source leaves

In order to shed light on the metabolic shift described above, the activity of enzymes of carbohydrate metabolism was measured in source leaves and ripe fruits harvested in the middle of the light period. In photosynthetic tissues, the activities of phosphoglucomutase (PGM), invertases (acid -AI- and neutral -NI-) and hexokinases (both fructokinase and glucokinase) showed significant decreased levels, whereas a higher activity of ADP-glucose pyrophosphorylase (AGPase) was observed (Table 2). By contrast, in mature fruits only a few alterations were observed; PGM showed a noteworthy increment whilst a mild increase trend was detected for invertase activities. The dramatic alteration in enzymatic activities revealed in source leaves lead us to investigate the status of trioses (trioses-P) and hexoses (hexoses-P) phosphate intermediates (Table 3). Strikingly, glucose-6-phosphate (Glu6P), fructose-6-phosphate (Fru6P), glucose-1-phosphate (Glu1P), glyceraldehyde-3-phosphate (3PGA) and dihydroxyacetone phosphate (DHAP) contents in *SPA*-silenced plants were remarkably higher than in wild-type controls. These results offer compelling evidence that *SPA* participates in source-sink carbon partitioning by upregulating the conversion of fixed carbon to exportable sugars.

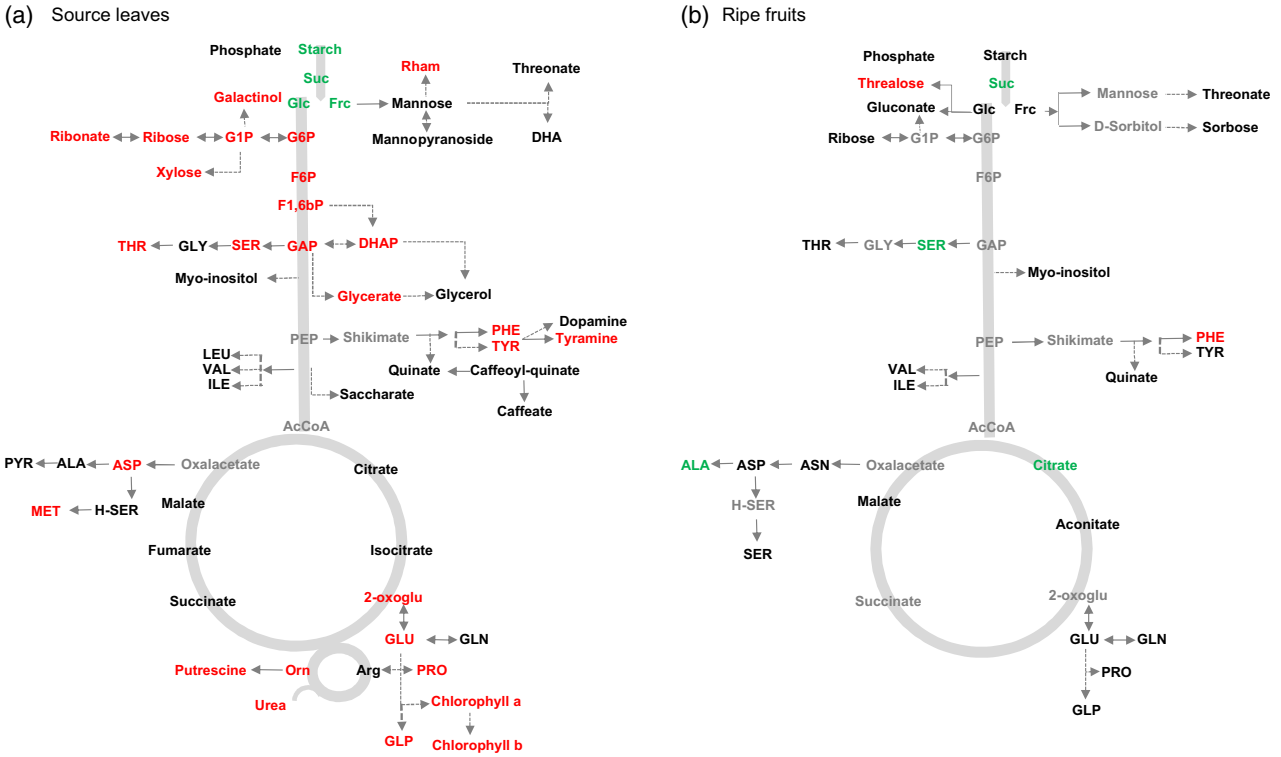

Figure 4. Changes in metabolite profiles from *SPA*-silenced transgenic lines.
Relative metabolite contents in source leaves (a) and ripe fruits (b). Metabolites are marked in green and red depict statistically significant reduction or increment, respectively, with respect to wild-type controls (cv. MoneyMaker) in at least two transgenic lines. Metabolites in black and gray indicate no differences or not measured, respectively.

Table 1 Pigment contents in *SPA*-silenced transgenic lines

	RNAi:*SPA*-7	RNAi:*SPA*-12	RNAi:*SPA*-39	RNAi:*SPA*-43	WT
Pigment contents in leaves (μg cm^{-2} tissue)					
Chlorophyll a	139.87 ± 4.50[a]	134.04 ± 4.75[a]	126.89 ± 5.28	128.25 ± 4.45	111.59 ± 4.86
Chlorophyll b	41.21 ± 1.94[a]	39.01 ± 0.80[a]	37.57 ± 1.58	38.33 ± 0.96[a]	31.30 ± 1.97
Carotenoids	41.37 ± 1.94[a]	38.49 ± 1.56[a]	37.32 ± 1.42	38.39 ± 0.28[a]	31.69 ± 1.32
Pigment contents in ripe fruits (mg per 100 g fresh weight)					
β-carotene	0.40 ± 0.04	0.34 ± 0.02	0.38 ± 0.05	0.43 ± 0.11	0.37 ± 0.02
Lycopene	5.22 ± 0.84	3.71 ± 0.48	4.35 ± 0.74	4.96 ± 1.09	4.44 ± 0.29

Pigment contents were determined by spectrophotometry. Values indicate means from three and six biological replicates in ripe fruits and source leaves, respectively.
[a]Significant differences against wild-type controls ($P < 0.05$).

DISCUSSION

Sugar partitioning-affecting (*SPA*), which encodes a DnaJ domain containing protein, was initially identified as a candidate gene associated with a pathway QTL described in an *S. pennellii* IL population, mapping to tomato chromosome 4 (Bermúdez *et al.*, 2008). In this work, we performed a functional characterization of this gene to evaluate its role both at physiological and biochemical levels. The primary protein structures displayed two non-synonymous substitutions, which resulted in different lengths of the predicted chloroplast TP, being shorter in the *S. pennellii* allele. Confocal microscopy imaging, however, did not show any difference between the localization of the different allele's products. Western blot analysis of chloroplast fractions demonstrated that the cultivated SPA protein is localized to the thylakoid membrane in agreement with the presence of a TM domain. Hence, the chloroplast localization suggested its involvement in plastidial metabolism that, as the major site of amino acid biosynthesis, is in accordance with the associated QTL for amino acids contents described by Schauer *et al.* (2006) and Schauer and Fernie (2006). Moreover, the tissue expression profile

Table 2 Carbohydrate metabolism enzymes activities in *SPA*-silenced transgenic lines

	RNAi:*SPA*-7	RNAi:*SPA*-12	RNAi:*SPA*-39	RNAi:*SPA*-43	WT
Enzyme activity in leaves (nmol min^{-1} g^{-1} FW)					
PGM	5817.3 ± 400.3[a]	5596.8 ± 594.2[a]	5723.9 ± 609.9[a]	6017.2 ± 431.8[a]	6674.2 ± 525.1
NI	89.7 ± 10.2[a]	81.5 ± 12.7[a]	102.1 ± 14.1[a]	95.6 ± 16.3[a]	138.2 ± 15.5
AGPase	5996 ± 234.9[a]	4426.2 ± 384.5[a]	5880.8 ± 267.2[a]	6215.1 ± 155.4[a]	5439.1 ± 268.8
G6PDH	62.6 ± 5.7	59.7 ± 7.4	67.81 ± 8.18	66.3 ± 9.5	64.7 ± 5.5
FK	154.3 ± 12.3[a]	140.4 ± 19.31[a]	137.7 ± 19.7[a]	135.9 ± 12.3[a]	176.8 ± 19.2
GK	64.2 ± 6.9[a]	61.8 ± 8.7[a]	67.01 ± 8.9[a]	69.3 ± 8.9[a]	92.8 ± 8.5
SuSy	301.1 ± 23.8	286.2 ± 17.2	306.1 ± 28.4	290.9 ± 22.5	302.4 ± 22.3
AI	124.9 ± 10.4[a]	107.7 ± 15.1[a]	105.3 ± 12.7[a]	105.3 ± 14.4[a]	167.6 ± 16.2
Enzyme activity in ripe fruits (nmol min^{-1} g^{-1} FW)					
PGM	635.1 ± 34.8[a]	607.4 ± 38.7[a]	604.9 ± 30.6[a]	425.3 ± 31.0	486.5 ± 27.1
NI	374.1 ± 10.3[a]	350.4 ± 29.4[a]	322.6 ± 20.1	305.2 ± 19.4	273.2 ± 16.5
AGPase	765.2 ± 17.5	756.6 ± 17.7	732.1 ± 20.8	637.4 ± 14.8	743.3 ± 17.7
G6PDH	40.2 ± 3.6	38.8 ± 2.3	35.6 ± 2.8	30.6 ± 2.9	38.4 ± 2.4
FK	16.9 ± 2.2	28.3 ± 4.9	19.4 ± 4.6	32.7 ± 6.7	16.3 ± 0.7
GK	5.4 ± 0.4	5.6 ± 0.7	4.9 ± 0.4	4.4 ± 0.4	7.1 ± 1.2
SuSy	391.4 ± 19.8	409.2 ± 11.8	398.4 ± 7.0	342.1 ± 6.0[a]	398.2 ± 10.6
AI	63.1 ± 3.5	54.7 ± 2.8	72.9 ± 3.0[a]	60.5 ± 2.0	57.4 ± 2.5

PGM, phosphoglucomutase; NI, neutral invertase; AGPase, ADP-glucose pyrophosphorylase; G6PDH, glucose-6-phosphate dehydrogenase; FK, fructokinase; GK, glucokinase; SuSy, sucrose synthase; AI, acid invertase.
Values indicate means from six biological replicates.
[a]Significant differences against wild-type controls ($P < 0.05$).

Table 3 Sugars phosphate contents in leaves from *SPA*-silenced transgenic lines

	RNAi:*SPA*-7	RNAi:*SPA*-12	RNAi:*SPA*-39	RNAi:*SPA*-43	WT
Hexoses-P (μmol g^{-1} DW)					
Glucose-6P	3.45 ± 0.17[a]	3.98 ± 0.20[a]	2.42 ± 0.15[a]	3.16 ± 0.19[a]	0.53 ± 0.04
Fructose-6P	0.79 ± 0.09[a]	0.89 ± 0.03[a]	0.84 ± 0.11[a]	0.96 ± 0.10[a]	0.24 ± 0.06
Glucose-1P	0.78 ± 0.08[a]	0.76 ± 0.08[a]	0.67 ± 0.09[a]	0.79 ± 0.09[a]	0.12 ± 0.05
Trioses-P (nmol g^{-1} DW)					
DHAP	17.3 ± 1.12[a]	19.5 ± 0.89[a]	21.8 ± 0.87[a]	26.4 ± 1.23[a]	12.6 ± 0.73
GAP	15.3 ± 0.85[a]	17.3 ± 0.24[a]	16.3 ± 0.79[a]	18.1 ± 1.09[a]	9.8 ± 0.54

DHAP, dihydroxyacetone phosphate; GAP, glyceraldehyde 3-P.
Values indicate means from six biological replicates in source leaves.
[a]Significant differences against wild-type controls ($P < 0.05$).

revealed that *SPA* mRNA is expressed preferentially in source leaves compared with any of the other organs tested and that the *S. lycopersicum* allele accumulates to significantly higher levels compared with the *S. pennellii* allele. Results obtained in promoter–GUS fusion expression experiments, together with the presence of an enhancer motif in the promoter region of *S. lycopersicum* allele, suggested that the observed differences in *SPA* mRNA accumulation were due to differential transcriptional activity. However, it cannot be ruled out that other transcriptional or post-transcriptional mechanism(s) contribute to *SPA* regulation.

Beyond an understanding of the molecular mechanism that underlie the traits observed in IL4-4, we were also interested in the biological function of *SPA per se*. DnaJ chaperones include a broad spectrum of protein structures and associated functions. Arabidopsis AtJ proteins are characterized by the presence of a J-domain and have been shown to be involved in H^+-ATPase regulation (Yang *et al.*, 2010), photosystem II (PSII) stabilization and stress-related transcription factor interaction (Chen *et al.*, 2010). However, tomato SPA protein lacks the J-domain but contains a zinc-finger domain and a TP. Chaperones with this same structure have been reported to act in plastid metabolism. Lu *et al.* (2006) demonstrated that a mutation on a cauliflower locus that encoded a member of this family (*Or* locus) determined proplastid differentiation into chromoplasts, and accumulated carotenoids in cauliflower inflorescences. In tobacco, Ham *et al.* (2006) identified TSIP1 (*Tobacco Stress-Induced1-Interacting Protein*), an envelope protein that is recruited by TSI1 transcription factor, thereby activating expression of stress-related genes. An Arabidopsis *SPA* ortholog, LQY1, has been described recently as a stroma-exposed thylakoid membrane protein.

Lqy1 mutants have been identified as mutants that failed to acclimate to photoinhibitory light conditions. Under high light stress, PSII repair and reassembly involve the breakage and formation of disulfide bonds among PSII proteins and, interestingly, it was demonstrated that the recombinant LQY1 protein had disulfide isomerase activity. However, under normal growth conditions, *lqy1* plants showed a wild-type phenotype. This evidence led the authors to conclude that, in Arabidopsis, LQY1 function is associated to PSII complex maintenance in light stressful conditions (Lu *et al.*, 2011).

Strikingly, our data with tomato silenced lines revealed that, under normal light growing conditions, SPA had a significant role in primary metabolism. *SPA*-silenced plants showed four to five times higher harvest indices, a trait of high economic importance. Transgenic plants produced more and heavier fruits but neither developmental nor morphological alterations were evidenced. These phenomena point to an increased sink strength of the fruits. The fact that no alteration in photosynthetic parameters was observed in source leaves from *SPA*-silenced plants (also not when expressed as total carbon assimilation per plant) together with the lower contents of leaf soluble sugars and starch, supported the hypothesis of an enhanced carbon export in the transgenics. In this sense, our data indicated that, in the leaves, the traffic of trioses-P from chloroplast to cytosol is elevated and results eventually in an increase in the cytosolic hexoses-P pool, which subsequently drives the metabolic flux towards sucrose synthesis and which is able to immediately leave the source cells (Smith and Stitt, 2007; Chiou and Bush, 1998). This scenario is in agreement with the reduced activity of invertases and PGM detected in the source leaves of the transgenic lines. The reduction in hexose kinases and the increase in AGPase activities are less intuitive. However, considerable evidence exists that both enzyme types are subject to transcriptional control (Müller-Röber *et al.*, 1990; Jang *et al.*, 1997).

The reduction in *SPA* mRNA also led to a dramatic increase in the amino acid contents of the source leaves. Total amino acid content was always correlated negatively to the sucrose content. Whilst at first sight it is difficult to understand the benefit of enhancing amino acid biosynthesis in carbohydrate-limiting conditions, this relationship has been well documented (Roessner-Tunali *et al.*, 2003). It has been postulated that increasing amino acid contents is a mechanism to compensate cellular osmolarity caused by the reduction in sucrose concentration (Fernie *et al.*, 2002). Alternatively, amino acid accumulation could be a means of nitrogen storage to be used when carbon becomes available (Smith and Stitt, 2007) or even the result of enhanced protein degradation to support mitochondrial respiration (Araújo *et al.*, 2011). It is important to note that the increment in glutamate content observed in the *SPA*-silenced plants could potentially explain the higher photosynthetic pigments accumulation, as this amino acid is the first precursor for tetrapyrrole ring biosynthesis. Thus, an increase in its production may lead to an elevated flux towards chlorophyll accumulation (von Wettstein *et al.*, 1995).

Conversely to the situation observed in source leaves, the comprehensive analysis of the metabolic and enzymatic profile of *SPA*-silenced fruit showed no major alteration. Nevertheless, it is worth to note the increased level of trehalose and the reduced sucrose content observed. In this regard, trehalose has emerged as an important regulatory metabolite in plants, involved in sucrose sensing (Paul *et al.*, 2008) and associated with a hyper-accumulation of starch (Rolland *et al.*, 2006). This statement is in agreement with the sucrose reduction and the starch-increasing trend observed in the transgenic fruits.

In summary, a role for the SPA protein can be proposed in coordinating sink-source balance through a trioses-P-dependent mechanism most probably via regulation of their transport. Despite a lack of direct evidence to date, it is tempting to speculate that SnRKs participate in the underlying regulatory network. It is well documented that these proteins co-ordinate carbon and nitrogen metabolism, inhibiting nitrate reductase (NR) and sucrose phosphate synthase (SPS; Paul and Foyer, 2001) and are inhibited by 3PGA (Piattoni *et al.*, 2011). The observed altered levels of this triose-P in the *SPA*-silenced lines might well, therefore, lead to the higher levels of amino acids displayed by these plants.

A comparative analysis of the fruit metabolite profile of *SPA*-silenced plants to that of the IL4-4 (carrying the *Sp-SPA* wild allele; Schauer *et al.*, 2006) showed that out of the 18 commonly quantified metabolites, only citrate, alanine, sucrose and trehalose were altered in both profiles. Bearing in mind that the introgressed region spans 11 cM, our results suggested that, even if the *SPA* locus may be contributing to the pathway QTL associated to this region, it is not the major determinant. However, the alteration in HI recorded in the *SPA*-silenced plants is in agreement with the fact that this trait is linked to this genomic region.

Whilst the above observations require further investigation, the results presented here reveal clearly an intriguingly function for the chaperone-like protein. Two hypotheses could be postulated in order to synthesize our understanding of the function of SPA and LQY1 in *S. lycopersicum* and *A. thaliana*, respectively. Firstly, although *SPA* and *LQY1* are ortholog genes, the encoding proteins may have undergone functional speciation. This situation is, by no means unlikely, given that, as determined from fossil evidence, tomato and Arabidopsis diverged early in dicotyledonous radiation (120 MYA; Bell *et al.*, 2005; Magallon and Sanderson, 2005). Due to the highly contrasting environments where these two species originated,

especially with regard to irradiance conditions (Peralta and Spooner, 2007), it is probable that tomato developed extra mechanisms for avoiding light stress. In this sense, SPA/LQY1 homologs are present in land plants but are absent from sequenced genomes of green algae and cyanobacteria, a situation that may reflect plant adaptation to excess light stress during the transition to land (Lu, 2011). Moreover, the deep morphological differences between Arabidopsis and tomato result in distinct source-sink relationships between the species (Carrari and Fernie, 2006). Secondly, SPA/LQY1 potentially operates as a bi-functional protein involved in sugar partitioning and PSII stabilization in both species. An example of a bi-functional protein has been already described in tomato. HSP21, a chloroplast small heat shock protein, participates both in fruit development under normal growth conditions and acts as a protectant under conditions of stress (Neta-Sharir *et al.*, 2005). In either case, the role of the tomato SPA protein under high light stressing conditions would require further experiments under altered light regimes, experiments that are less trivial to achieve in tomato due simply to the size of the plant.

In the global context of a growing population, which is expected to reach 9.2 billion by 2050, food production has become a main concern worldwide. Moreover, climate change and the need for biofuel platform enhancement add another challenge for plant genetic engineering. An understanding of source-sink control mechanisms is an important bottleneck for improvement biomass generation. Here, we demonstrate that the SPA protein participates in the control of source-sink carbon distribution in tomato. As this function was not reported previously for this protein family, it thus follows that this protein is a noteworthy target for plant biomass engineering.

EXPERIMENTAL PROCEDURES

Plant material and growth conditions

Tomato, *Solanum lycopersicum* L. (cv. MoneyMaker), and *Nicotiana benthamiana* seeds were obtained from Meyer Beck (Berlin, Germany). *S. lycopersicum* (inbred variety M82, Acc LA3475) and IL 4-4 were kindly provided by C.M. Rick, Tomato Genetics Resource Center (TGRC). Plants were grown under greenhouse conditions: 16 h/8 h photoperiod, 24 $\pm$ 3°C, 60% humidity and 140 $\pm$ 40 μmol m^{-2} sec^{-1} incident photo-irradiance in 20-L and 1-L pots for tomato and *N. benthamiana*, respectively. Tomato source leaves were sampled from second or third leaflets of the third totally expanded leaf of 4-week-old plants. Mature green and ripe fruits were collected at 37 or 52 days after anthesis, respectively. Stem samples were obtained from the fourth internode. All experiments were performed with 4–8 plants per genotype as biological replicates.

DNA sequence analysis

The *Solanum pennellii* allele sequence of *SPA* was obtained from chromosome 4 C04SpBP093E005.P4C04 (FJ809740) BAC clone (83 193 bp); while the ortholog *Solanum lycopersicum* sequence was identified from LE_HBa-331L22 (CU222538) clone (100 572 bp; Kamenetzky *et al.*, 2010).

For phylogenetic analysis, a survey at NCBI and literature of previously functional characterized DnaJ homologs in plants was performed. *A. thaliana* LQY1 (NM_106220) was taken from Lu *et al.* (2011); *N. tabacum* TSIP1 (AAD18030) and *A. thaliana* TSIP1 (AC006585) from Ham *et al.* (2006); *B. oleracea* OR (ABH07405), *S. lycopersicum* OR (TA6503_4081) and *A. thaliana* OR (NM_203246) from Lu *et al.* (2006); *A. thaliana* Atj3 (AY113878) and *A. thaliana* Atj8 (AF332461) from Chen *et al.* (2010, 2011). Atj3 and Atj8 orthologs from *S. lycopersicum*, Slj3 (SGN-U578090) and Slj8 (SGN-U580038) were identified as the best hits for the respective *A. thaliana* sequences. The predicted amino acid sequences were aligned using CLUSTALW multiple alignment (version 1.5; Thompson *et al.*, 1994). The phylogenetic tree was constructed with the neighbor-joining method with the MOLECULAR EVOLUTIONARY GENETICS ANALYSIS (MEGA) program (Tamura *et al.*, 2007). The evolutionary distances were computed using the JTT matrix-based method (Jones *et al.*, 1992) and are in the units of the number of amino acid substitutions per site. The bootstrap values were determined from 1000 trials. Prediction of sub-cellular localization of proteins was performed with the TargetP server (http://www.cbs.dtu.dk/services/TargetP/; Emanuelsson *et al.*, 2000). Prediction of transmembrane domains was performed using the TMHMM server (http://www.cbs.dtu.dk/services/TMHMM/; Krogh *et al.*, 2001).

The intergenic region upstream *SPA* was considered as putative regulatory region and analyzed to identify differential motifs for both alleles using PLACE (Higo *et al.*, 1999) and PLANTCARE (Lescot *et al.*, 2002) databases.

Chloroplast fractionation

Percoll-purified chloroplast fractions were obtained from 30 g of fresh tomato leaves (cv. MoneyMaker) as described by Stöckel and Oelmüller (2004).

Protein analysis

Western blot analysis was performed in accordance with Sambrook *et al.* (1989) using polyclonal antibodies against SPA protein (LQY1/SPA, 10 kDa) at 1:1000 dilution, kindly provided by Dr Robert Last. The antibodies against chloroplastic photosystem II/D1 (psbA/D1, 32 kDa) control protein were purchased from Agrisera (Agrisera Antibodies, Vännäs, Sweden, http://www.agrisera.com) and used at 1:10 000 dilution.

Light and transmission electron microscopy

Source leaves and fruits were fixed with 2.5% glutaraldehyde in 0.1 M sodium phosphate buffer pH 7.2, post-fixed in 2% osmium tetroxide in 0.1 M sodium phosphate buffer pH 7.2, post-treated with 1% tannic acid in 0.05 M sodium phosphate buffer pH 7.2, dehydrated in a graded acetone series and embedded in Spurr resin. Semi-thin sections were treated with Lugol's solution (Johansen, 1940) and analyzed with an Olympus BX41 light microscope to identify starch granules. To observe plastid ultrastructure, ultrathin sections were counterstained with uranyl acetate (Watson, 1958) and lead citrate (Reynolds, 1963), followed by analysis with a Zeiss EM 900 transmission electron microscope.

Cloning procedures

The constructs for sub-cellular localization, promoter activity and transgenic plant generation were obtained in pK7FWG2, pHGWFS7 and p7GWIWG2(I) binary vectors (Karimi *et al.*, 2002), respectively. Procedures were followed as described by de Godoy

et al. (2013). For specific fragment amplification the primers used are detailed in Table S5.

Agroinfiltration for promoter analyses and sub-cellular localization

For promoter analyses and sub-cellular localization experiments pKGWFS7_*SPA*_PromLyc, pKGWFS7_*SPA*_PromPen, pKGWFS7_35S, pKGWFS7_empty, pK7FWG2-SPA::GFP_lyc and pK7FWG2-SPA::GFP_pen were introduced into *Agrobacterium tumefaciens* strain GV3101. Infiltration in *N. benthamiana* leaves and confocal visualization were performed as described by de Godoy *et al.* (2013). For promoter analyses, histochemical detection of GUS activity was performed as described by Jefferson *et al.* (1987).

RNA isolation and qPCR analyses

RNA extraction and qPCR experiments were carried out in accordance with de Godoy *et al.* (2013). The primers used are detailed in Table S5.

Generation of transgenic plants

The pK7GWIWG2(I)_*SPA* construct was used to transform tomato (*S. lycopersicum* cv. MoneyMaker) via *Agrobacterium tumefaciens* as described previously by Tauberger *et al.* (2000). The screening of 27 T0 transgenic lines was performed as described by de Godoy *et al.* (2013). Four lines were chosen for further detailed phenotypic characterizations which were subsequently tested for their levels of *SPA* silencing both in T0 and T1 generations. Progeny tests were performed on T1 seeds and displayed segregation ratios of 3:1 (resistance:susceptibility to 100 μg ml^{-1} kanamycin) suggesting a single copy insertion of the transgene. T1 plants obtained after selection in kanamycin-containing medium were transferred to the greenhouse and used for further experiments.

Photosynthetic parameter measurements

Photosynthetic parameters, including gas exchange and chlorophyll fluorescence emission were determined as described in de Godoy *et al.* (2013) in T0 transgenic plants.

Pigment quantification

Pigments were quantified in T0 transgenic plants. Carotenoids and chlorophyll extraction and quantification for green tissues (leaves and mature green fruits) were performed according to protocols described by Lichtenthaler (1987). β-Carotene and lycopene extraction and quantification for ripe fruits were performed in accordance with Heredia *et al.* (2009).

Sugars and starch quantification

Sugars and starch content were determined spectrophotometrically in T0 and T1 generation transgenic lines in accordance with Dominguez *et al.* (2013).

Metabolite analysis

For metabolite analysis in T0 lines, the extraction, derivatization, standard addition, and sample injection for GC-MS were performed in accordance with Lisec *et al.* (2006) and Osorio *et al.* (2012). Identification and quantification of the compounds were performed with TAGFINDER 4.0 software and the mass spectra were cross-referenced with those in the Golm Metabolome Database (Kopka *et al.*, 2005; Schauer *et al.*, 2005). Three to six biological replicates were used for this analysis.

Enzyme assays

Sample extraction, handling, and enzyme activity determination were performed in T1 transgenic plants exactly as described by Steinhauser *et al.* (2010).

Sugar phosphate quantification

Sugar phosphate intermediates were measured in source leaves and mature fruits harvested from T1 transgenic plants. The extraction procedure was performed as follows: 0.6 ml of MeOH + HCl_3 (2:1 v/v) was added to the dried samples (10–30 mg). The mixture was sonicated at 8°C for 25 min. Later, 0.4 ml of H_2O was added to each vial. The vials were then centrifuged at 4°C and 10 000 ***g*** for 10 min. Hexoses-P and trioses-P were analyzed from the polar phase. Glc6P, Glc1P and Fru6P contents were determined successively in each extract by enzyme-based spectrophotometric assay of $NADP^+$ reduction at 340 nm. Aliquots of 10–30 μl of extracts were used for Glc6P, Fru6P and Glc1P determinations. The reaction was performed in a total volume of 600 μl that contained 100 mM Tris pH 8.1, 5 mM $MgCl_2$, 0.12 mg $NADP^+$. Then, 0.14 U of Glc6P dehydrogenase, 0.7 U of phosphoglucose isomerase, and 0.4 U of phosphoglucomutase were added sequentially for Glc6P, Glc1P, and Fru6P determinations.

DHAP and 3PGA contents were determined successively in each extract by enzyme-based spectrophotometric assay of NADH oxidation at 340 nm. Aliquots of 100 μl of extracts were used and the reaction was performed in a total volume of 600 μL containing 100 mM Tris, pH 8.1, 5 mM $MgCl_2$, 0.01 mg NADH. Then, 0.3 U of glyceraldehyde-3-P dehydrogenase, and 0.6 U of triose-P isomerase were added sequentially.

Statistical analyses

Data on transgenic lines characterization were analyzed statistically in accordance with Sokal and Rohlf (1995). When the pool of data presented homoscedasticity, an analysis of variance (ANOVA) followed by a Tukey or Duncan test ($P < 0.05$) was used. Due to lack of homoscedasticity, a non-parametric comparison was also performed by Kruskal–Wallis test ($P < 0.05$). Statistical tests were performed with INFOSTAT software (Di Rienzo *et al.*, 2011). qPCR data were analyzed with LINREGPCR software (Ruijter *et al.*, 2009) to obtain C_t values and primer efficiency. Relative expression and statistics analysis were calculated using fgStatistics software (Di Rienzo, 2009).

ACKNOWLEDGEMENTS

This work was supported partially with grants from FAPESP, CNPq and USP (Brazil); Max Planck Society (Germany); INTA, CONICET and ANPCyT (Argentina); and under the auspices of the EU SOL Integrated Project FOOD-CT-2006-016214. L.B, F.G and J.A. were recipient of FAPESP fellowships. M.R. hold fellowship from CNPq. F.C. and R.A. are members of CONICET (Argentina). We thank D. Prodhomme (INRA Bordeaux, France) for technical assistance. S.O. acknowledges the support by Ministerio de Ciencia e Innovación, Spain (Ramón and Cajal contract). This work was carried out in compliance with current laws governing genetic experimentation in Brazil and Argentina.

SUPPORTING INFORMATION

Additional Supporting Information may be found in the online version of this article.

Figure S1. Photomicrographs of leaves and ripe fruits stained with Lugol's solution.

Figure S2. Transmission electronic microscopy micrographs of source leaves.

Table S1. Differential *cis*-regulatory motifs found in the promoter regions of *S. lycopersicum* and *S. pennellii SPA* alleles.

Table S2. Leaf metabolite profile of SPA-silenced lines.

Table S3. Fruit metabolite profile of SPA-silenced lines.

Table S4. Photosynthetic and chlorophyll fluorescence parameters measured in 4 week-old plants.

Table S5. Primers used for each experiment.

REFERENCES

Araújo, W.L., Tohge, T., Ishizaki, K., Leaver, C.J. and Fernie, A.R. (2011) Protein degradation - an alternative respiratory substrate for stressed plants. *Trends Plant Sci.* **16**, 489–498.

Bell, C.D., Soltis, D.E. and Soltis, P.E. (2005) The age of the angiosperms: a molecular timescale without a clock. *Evolution*, **59**, 1245–1258.

Bermúdez, L., Urias, U., Milstein, D., Kamenetzky, L., Asis, R., Fernie, A.R., Van Sluys, M.A., Carrari, F. and Rossi, M. (2008) A candidate gene survey of quantitative trait loci affecting chemical composition in tomato fruit. *J. Exp. Bot.* **59**, 2875–2890.

Carrari, F. and Fernie, A.R. (2006) Metabolic regulation underlying tomato fruit development. *J. Exp. Bot.* **57**, 1883–1897.

Carrari, F., Baxter, C., Usadel, B. *et al.* (2006) Integrated analysis of metabolite and transcript levels reveals the metabolic shifts that underlie tomato fruit development and highlight regulatory aspects of metabolic network behavior. *Plant Physiol.* **142**, 1380–1396.

Chen, K.M., Holmström, M., Raksajit, W., Suorsa, M., Piippo, M. and Aro, E.M. (2010) Small chloroplast-targeted DnaJ proteins are involved in optimization of photosynthetic reactions in *Arabidopsis thaliana*. *BMC Plant Biol.* **7**, 10–43.

Chen, K.M., Piippo, M., Holmström, M., Nurmi, M., Pakula, E., Suorsa, M. and Aro, E.M. (2011) A chloroplast-targeted DnaJ protein AtJ8 is negatively regulated by light and has rapid turnover in darkness. *J. Plant Physiol.* **168**, 1780–1783.

Chiou, T.J. and Bush, D.R. (1998) Sucrose is a signal molecule in assimilate partitioning. *Proc. Natl. Acad. Sci. USA.* **14**, 4784–4788.

Di Rienzo, J.A. (2009) *Statistical Software for the Analysis of Experiments of Functional Genomics*. Argentina: RDNDA. http://sites.google.com/site/fgStatistics/.

Di Rienzo, J.A., Casanoves, F., Balzarini, M.G., Gonzalez, L., Tablada, M. and Robledo, C.W. (2011) *InfoStat Versión 2011*. Argentina: Grupo InfoStat, FCA, Universidad Nacional de Córdoba. URL http://www.infostat.com.ar.

Dominguez, P.G., Frankel, N., Mazuch, J., Balbo, I., Iusem, N.D., Fernie, A.R. and Carrari, F. (2013) Asr1 mediates glucose-hormone crosstalk by affecting sugar trafficking in tobacco plants. *Plant. Physiol.* **161**, 1486–1500.

Dorn, K.V., Willmund, F., Schwarz, C. *et al.* (2010) Chloroplast DnaJ-like proteins 3 and 4 (CDJ3/4) from *Chlamydomonas reinhardtii* contain redox--active Fe-S clusters and interact with stromal HSP70B. *Biochem. J.* **427**, 205–215.

Emanuelsson, O., Nielsen, H., Brunak, S. and von Heijne, G. (2000) Predicting subcellular localization of proteins based on their N-terminal amino acid sequence. *J. Mol. Biol.* **300**, 1005–1016.

Eshed, Y. and Zamir, D. (1995) An introgression line population of *Lycopersicon pennellii* in the cultivated tomato enables the identification and fine mapping of yield-associated QTL. *Genetics*, **141**, 1147–1162.

Fernie, A.R., Tiessen, A., Stitt, M., Willmitzer, L. and Geigenberger, P. (2002) Altered metabolic fluxes result from shifts in metabolite levels in sucrose phosphorylase expressing potato tubers. *Plant Cell Environ.* **25**, 1219–1232.

de Godoy, F., Bermúdez, L., Silvestre, B.L. *et al.* (2013) Galacturonosyltransferase 4 silencing alters pectin composition and carbon partitioning in tomato. *J. Exp. Bot.* **64**, 2449–2466.

Ham, B.K., Park, J.M., Lee, S.B., Kim, M.J., Lee, I.J., Kim, K.J., Kwon, C.S. and Paek, K.H. (2006) Tobacco Tsip1, a DnaJ-type Zn finger protein, is recruited to and potentiates Tsi1-mediated transcriptional activation. *Plant Cell*, **18**, 2005–2020.

Heredia, A., Peinado, I., Barrera, C. and Grau, A.A. (2009) Influence of process variables on color changes, carotenoids retention and cellular tissue alteration of cherry tomato during osmotic dehydration. *J. Food Compost. Anal.* **22**, 285–294.

Higo, K., Ugawa, Y., Iwamoto, M. and Korenaga, T. (1999) Plant *cis*-acting regulatory DNA elements (PLACE) database. *Nucleic Acids Res.* **27**, 297–300.

Jang, J.C., León, P., Zhou, L. and Sheen, J. (1997) Hexokinase as a sugar sensor in higher plants. *Plant Cell*, **9**, 5–19.

Jefferson, R.A., Kavanagh, T.A. and Bevan, M.W. (1987) GUS fusions: beta-glucuronidase as a sensitive and versatile gene fusion marker in higher plants. *EMBO J.* **6**, 3901–3907.

Johansen, D.A. (1940) *Plant Microtechnique*. New York, NY: McGraw-Hill.

Jones, D.T., Taylor, W.R. and Thornton, J.M. (1992) The rapid generation of mutation data matrices from protein sequences. *Comput. Appl. Biosci.* **8**, 275–282.

Kamenetzky, L., Asís, R., Bassi, S. *et al.* (2010) Genomic analysis of wild tomato introgressions determining metabolism- and yield-associated traits. *Plant Physiol.* **152**, 1772–1786.

Karimi, M., Inzé, D. and Depicker, A. (2002) GATEWAY™ vectors for Agrobacterium-mediated plant transformation. *Trends Plant Sci.* **7**, 193–195.

Kopka, J., Schauer, N., Krueger, S. *et al.* (2005) GMD#CSB.DB: the GolmMetabolome Database. *Bioinformatics*, **21**, 1635–1638.

Krogh, A., Larsson, B., von Heijne, G. and Sonnhammer, E.L. (2001) Predicting transmembrane protein topology with a hidden Markov model: application to complete genomes. *J. Mol. Biol.* **305**, 567–580.

Lescot, M., Déhais, P., Moreau, Y., De Moor, B., Rouzé, P. and Rombauts, S. (2002) PlantCARE: a database of plant cis-acting regulatory elements and a portal to tools for *in silico* analysis of promoter sequences. *Nucleic Acids Res.* **30**, 325–327.

Li, J., Zhang, H., Hu, J., Liu, J. and Liu, K. (2012) A heat shock protein gene, CsHsp45.9, involved in the response to diverse stresses in cucumber. *Biochem. Genet.* **50**, 565–578.

Lichtenthaler, H.K. (1987) Chlorophylls and carotenoids: pigments of photosynthetic biomembranes. *Methods Enzymol.* **148**, 350–382.

Lippman, Z.B., Semel, Y. and Zamir, D. (2007) An integrated view of quantitative trait variation using tomato interspecific introgression lines. *Curr. Opin. Genet. Dev.* **17**, 545–552.

Lisec, J., Schauer, N., Kopka, J., Willmitzer, L. and Fernie, A.R. (2006) Gas chromatography mass spectrometry-based metabolite profiling in plants. *Nat. Protoc.* **1**, 387–396.

Lu, Y. (2011) The occurrence of a thylakoid-localized small zinc finger protein in land plants. *Plant Signal. Behav.* **6**, 1881–1885.

Lu, S., Van Eck, J., Zhou, X. *et al.* (2006) The cauliflower or gene encodes a Dnaj cysteine-rich domain-containing protein that mediates high levels of β-carotene accumulation. *Plant Cell*, **18**, 3594–3605.

Lu, Y., Hall, D.A. and Last, R.L. (2011) A small zinc finger thylakoid protein plays a role in maintenance of photosystem II in *Arabidopsis thaliana*. *Plant Cell*, **23**, 1861–1875.

Magallon, S.A. and Sanderson, M.J. (2005) Angiosperm divergence times: the effect of genes, codon positions, and time constraints. *Evolution*, **59**, 1653–1670.

Müller-Röber, B.T., Kossmann, J., Hannah, L.C., Willmitzer, L. and Sonnewald, U. (1990) One of two different ADP-glucose pyrophosphorylase genes from potato responds strongly to elevated levels of sucrose. *Mol. Gen. Genet.* **224**, 136–146.

Neta-Sharir, I., Isaacson, T., Lurie, S. and Weiss, D. (2005) Dual role for tomato heat shock protein 21: protecting photosystem II from oxidative stress and promoting color changes during fruit maturation. *Plant Cell*, **17**, 1829–1838.

Nunes-Nesi, A., Fernie, A.R. and Stitt, M. (2010) Metabolic and signaling aspects underpinning the regulation of plant carbon nitrogen interactions. *Mol. Plant*, **6**, 973–996.

Nunes-Nesi, A., Araújo, W.L. and Fernie, A.R. (2011) Targeting mitochondrial metabolism and machinery as a means to enhance photosynthesis. *Plant Physiol.* **155**, 101–107.

Osorio, S., Do, P.T. and Fernie, A.R. (2012) Profiling primary metabolites of tomato fruit with gas chromatography/mass spectrometry. *Methods Mol. Biol.* **860**, 101–109.

Paul, M.J. and Foyer, C.H. (2001) Sink regulation of photosynthesis. *J. Exp. Bot.* **52**, 1383–1400.

Paul, M.J. and Pellny, T.K. (2003) Carbon metabolite feedback regulation of leaf photosynthesis and development. *J. Exp. Bot.* **54**, 539–547.

Paul, M.J., Primavesi, L.F., Jhurreea, D. and Zhang, Y. (2008) Trehalose metabolism and signaling. *Annu. Rev. Plant Biol.* **59**, 417–441.

Peralta, I.E. and Spooner, D.M. (2007) History, origin and early cultivation of tomato (Solanaceae). In *Genetic Improvement of Solanaceous Crops*, Vol. 2 (Tomato) (Razdan, M.K. and Mattoo, A.K. eds). Enfield, CT: Science Publishers, pp. 1–27.

Piattoni, C.V., Bustos, D.M., Guerrero, S.A. and Iglesias, A.A. (2011) Non-phosphorylating glyceraldehyde-3-phosphate dehydrogenase is phosphorylated in wheat endosperm at Ser404 by a SNF1-related protein kinase allosterically inhibited by ribose 5 phosphate. *Plant. Physiol.* **156**, 1337–1350.

Reynolds, E.S. (1963) The use of lead citrate at high pH as an electron- opaque stain in electron microscopy. *J. Cell Biol.* **17**, 208–212.

Roessner-Tunali, U., Urbanczyk-Wochniak, E., Czechowski, T., Kolbe, A., Willmitzer, L. and Fernie, A.R. (2003) De novo amino acid biosynthesis in potato tubers is regulated by sucrose levels. *Plant Physiol.* **133**, 683–692.

Roitsch, T. (1999) Source-sink regulation by sugar and stress. *Curr. Opin. Plant Biol.* **2**, 198–206.

Rolland, F., Baena-González, E. and Sheen, J. (2006) Sugar sensing and signaling in plants: conserved and novel mechanisms. *Annu. Rev. Plant. Biol.* **57**, 675–709.

Ruijter, J.M., Ramakers, C., Hoogaars, W.M., Karlen, Y., Bakker, O., van den Hoff, M.J. and Moorman, A.F. (2009) Amplification efficiency: linking baseline and bias in the analysis of quantitative PCR data. *Nucleic Acids Res.* **37**, 45.

Sambrook, J., Fritsch, E.F. and Maniatis, T. (1989) *Molecular Cloning: A Laboratory Manual*, 2nd edn. Cold Spring Harbor: Cold Spring Harbor Laboratory Press.

Schauer, N. and Fernie, A.R. (2006) Plant metabolomics: towards biological function and mechanism. *Trends Plant Sci.* **10**, 508–516.

Schauer, N., Steinhauser, D., Strelkov, S. *et al.* (2005) GC-MS libraries for the rapid identification of metabolites in complex biological samples. *FEBS Lett.* **579**, 1332–1337.

Schauer, N., Semel, Y., Roessner, U. *et al.* (2006) Comprehensive metabolic profiling and phenotyping of interspecific introgression lines for tomato improvement. *Nat. Biotechnol.* **24**, 447–454.

Shimada, H., Mochizuki, M., Ogura, K., Froehlich, J.E., Osteryoung, K.W., Shirano, Y., Shibata, D., Masuda, S., Mori, K. and Takamiya, K. (2007) Arabidopsis cotyledon-specific chloroplast biogenesis factor CYO1 is a protein disulfide isomerase. *Plant Cell*, **19**, 3157–3169.

Smith, A.M. and Stitt, M. (2007) Coordination of carbon supply and plant growth. *Plant Cell Environ.* **30**, 1126–1149.

Sokal, R.R. and Rohlf, J.F. (1995) *Biometry: the Principles and Practice of Statistics in Biological Research*, 3rd edn. New York, NY: W.H. Freeman, p. 887.

Steinhauser, M.C., Steinhauser, D., Koehl, K., Carrari, F., Gibon, Y., Fernie, A.R. and Stitt, M. (2010) Enzyme activity profiles during fruit development in tomato cultivars and *Solanum pennellii*. *Plant Physiol.* **153**, 80–98.

Stöckel, J. and Oelmüller, R. (2004) A novel protein for photosystem I biogenesis. *J. Biol. Chem.* **279**, 10243–10251.

Tamura, K., Dudley, J., Nei, M. and Kumar, S. (2007) MEGA4: Molecular Evolutionary Genetics Analysis (MEGA) software version 4.0. *Mol. Biol. Evol.* **24**, 1596–1599.

Tauberger, E., Fernie, A.R., Emmermann, M., Renz, A., Kossmann, J., Willmitzer, L. and Trethewey, R.N. (2000) Antisense inhibition of plastidial-phosphoglucomutase provides compelling evidence that potato tuber amyloplasts import carbon from the cytosol in the form of glucose-6-phosphate. *Plant J.* **23**, 43–53.

Thompson, J., Higgins, D. and Gibson, T. (1994) CLUSTAL W: improving the sensitivity of progressive multiple sequence alignment through sequence weighting position-specific gap penalties and weight matrix choice. *Nucleic Acids Res.* **22**, 4673–4680.

Tilman, D., Balzer, C., Hill, J. and Befort, B.L. (2011) Global food demand and the sustainable intensification of agriculture. *Proc. Natl Acad. Sci. USA* **108**, 20260–20264.

Vitha, S., Froehlich, J.E., Koksharova, O., Pyke, K.A., van Erp, H. and Osteryoung, K.W. (2003) ARC6 is a J-domain plastid division protein and an evolutionary descendant of the cyanobacterial cell division protein Ftn2. *Plant Cell*, **15**, 1918–1933.

Watson, M.L. (1958) Staining of tissue sections for electron microscopy with heavy metals. *J. Biophys. Biochem. Cytol.* **4**, 475.

von Wettstein, D., Gough, S. and Kannangara, C.G. (1995) Chlorophyll biosynthesis. *Plant Cell*, **7**, 1039–1057.

Yang, J. and Zhang, J. (2010) Crop management techniques to enhance harvest index in rice. *J. Exp. Bot.* **61**, 3177–3189.

Yang, Y., Qin, Y., Xie, C. *et al.* (2010) The Arabidopsis chaperone J3 regulates the plasma membrane H+-ATPase through interaction with the PKS5 kinase. *Plant Cell*, **22**, 1313–1332.

